Metallic Iron in Basalts of the Malyi Yenisei Lava River: Results of Thermomagnetic Study

D. M. Pechersky[a], A. Yu. Kazansky[b], A. M. Kozlovsky[c], D. M. Kuzina[d], and G. P. Markov[a], *

[a]*Schmidt Institute of Physics of the Earth, Russian Academy of Sciences, Moscow, 123242 Russia*
[b]*Faculty of Geology, Moscow State University, Moscow, 119991 Russia*
[c]*Institute of Geology of Ore Deposits, Petrography, Mineralogy and Geochemistry,*
Russian Academy of Sciences, Moscow, 119017 Russia
[d]*Kazan Federal University, Kazan, 420008 Russia*
**e-mail: gpmarkov@yandex.ru*

Abstract—Thermomagnetic analysis of samples from two sections of lava layers of the Late Cenozoic basalt lava river in the Malyi Yenisei valley is carried out. The main magnetization carrier in the studied basalts is titanomagnetite with the Curie points of $100-120°C$ which is frequently substantially oxidized both single-phase and heterophase up to magnetite. It is likely that some part of metallic iron in the studied samples has also been oxidized and even disintegrated, which resulted in the significant scatter of iron concentration across the flow against which, however, the increasing trend of iron concentration in the lava flow from the top downwards is observed. The relative magnitude of this increase (iron concentration gradient along the vertical of the lava flow) is almost constant for all flows of the lava sequence probably indicating the decisive role of gravity in iron particle precipitation in the lava. Based on the synthesis of iron particle data from different objects and different regions of the world, this correlation with gravity also follows from the very similar shapes of particle size histograms of iron. This is most clearly seen from the same particle size modes ($10-20\,\mu m$). Another important finding is that this constant mode of iron particle size does not depend on age and origin of rock as well as on the type of particle source (terrestrial or extraterrestrial).

INTRODUCTION

Previously (Pechersky et al., 2018), the thermomagnetic study of basalts of Zhom-Bolok lava river, East Sayan, revealed a fairly natural although not quite obvious phenomenon: relatively heavy particles of metallic iron precipitate in liquid lava melt, which was confirmed by the detected increase in iron content from top to bottom in the lava flow. The average iron concentration over a series of sections of the Zhom-Bolok lava river in the lower part of the flows is several times higher than that in the upper part.

The composite diagram of iron content distribution along the vertical section of four Zhom-Bolok lava flows, which is presented in Fig. 1a, shows that despite wide scatter of the data, a quite distinct trend of iron concentration increasing from top to bottom is observed. A more visual picture of the changes in iron concentration along the vertical section of flows can be seen from the comparison of average iron concentrations in three parts of the section of flows—in the upper, middle, and lower ones(Fig. 1b).

In our opinion, the result obtained in (Pechersky et al., 2018) (Fig. 1) is definitely of interest to geophysics as it is likely to testify to the decisive role of Earth's gravity in the deposition of iron particles in a liquid basalt lava.

However, it should be noted that the number of basalt samples of Zhom-Bolok lava river selected from each flow was overall rather limited: two or three samples were taken from each flow (at the top, middle, and bottom). Therefore, the obtained results needed to be validated based on a more representative collection of basalt samples.

This work addresses the thermomagnetic study of metallic iron in basalt samples from the lava river of Malyi Yenisei.

STUDY OBJECT

The lava river of the Malyi Yenisei valley (Kaa-Khem and Kyzyl-Khem) is the largest Late Cenozoic valley lava flow of South Baikalian volcanic area of Central Asia (Yarmolyuk et al., 2004; 2015). Its length

(a)

Iron concentration, %

(b)
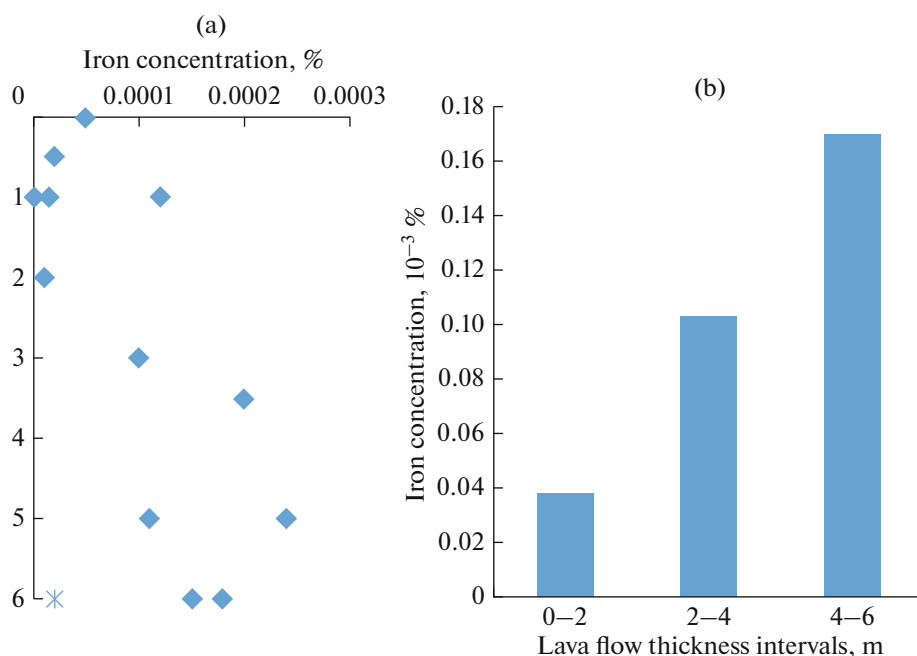
Fig. 1. (a) Composite distribution of iron concentrations along section and (b) mean iron concentration in top (0−2 m), middle (2−4 m), and bottom (4−6 m) parts of vertical section of four flows of Zhom-Bolok lava river.

is about 175 km (Fig. 2). The volcanic center is located in the upper reaches of Kyzyl-Khem River and is nowadays the remains of a scoria cone completely overlain by massive lavas. Lava flows are localized within a narrow V-shaped valley with a width rarely more than 2 km. At present, the lava stratum is fully cut through by the river along its entire length. In the basement of the lava terrace, the predominantly Early Paleozoic granitoids of the Kaakhem batholith are exposed. The total thickness of lava sequence varies from 350 m in the vicinity of the volcanic cone to 10−20 m at the lower and upper ends of the lava river. The thickness of individual flows varies from a few to 40 m. The boundaries of lava flows are clearly traced by the rather thin (a thickness up to 0.5 m) scoria zones in the top of the flows. At places, lava flows are separated by the horizons of alluvial sands. In the flows with a thickness of more than 15 m there are zones with different types of jointing: platy horizontal, vertical columnar, fan, and block. Obviously, this zoning corresponds to different rheology of lavas within thick flows.

Petrographically, volcanic rocks of the Malyi Yenisei (MYe) lava river correspond to porphyry olivine basalts. Olivine phenocrysts reach a size of 1.5 mm and make up about 10% of the rock volume. The groundmass is mainly well crystallized and consists of microlites of olivine, clinopyroxene, plagioclase, and titanomagnetite. At places, rocks with predominance of volcanic glass occur at the base of lava flows. The rock-forming minerals and volcanic glass are practically not affected by secondary alteration.

The age of lava flows was determined by K-Ar dating the groundmass of basalts sampled from the top and bottom parts of the lava sequence in the middle reaches of the lava river and estimated at 280 ± 40 and 260 ± 40 ka (Yarmolyuk et al., 2003).

Samples for thermomagnetic studies were acquired from two sections of lava sequence 33 km (I in Fig. 2) and 45 km (II in Fig. 2) km downstream from the volcanic center at the points with coordinates 51.3827° N, 97.3851° E and 51.3487° N, 97.2534° E, respectively. The samples were taken directly from the scarps of lava flows where the base and the top were clearly fixed, in the direction from the flow's bottom upwards at close intervals in thickness. The lower flows of the lava river are hidden under the talus, therefore sampling was possible only 50−80 m above the bottom of the lava sequence. In the first section in the mouth of Tuzhema River, from four flows (MYe-10/1, MYe-10/2, MYe-10/3 and MYe-10/4) with thicknesses 6, 15, 25 and 5 m, overall 6, 6, 9 and 6 samples were taken, respectively. In the second section, two thick flows MYe-10/5 and MYe-10/6 with a thickness of 20 and 36 m were sampled; 5 and 9 samples were taken, respectively.

STUDY TECHNIQUE

Metallic iron in basalt samples of the Malyi Yenisei lava river was studied by the well-known method of thermomagnetic analysis (TMA). In order to increase the reliability of the results, TMA of the selected basalt
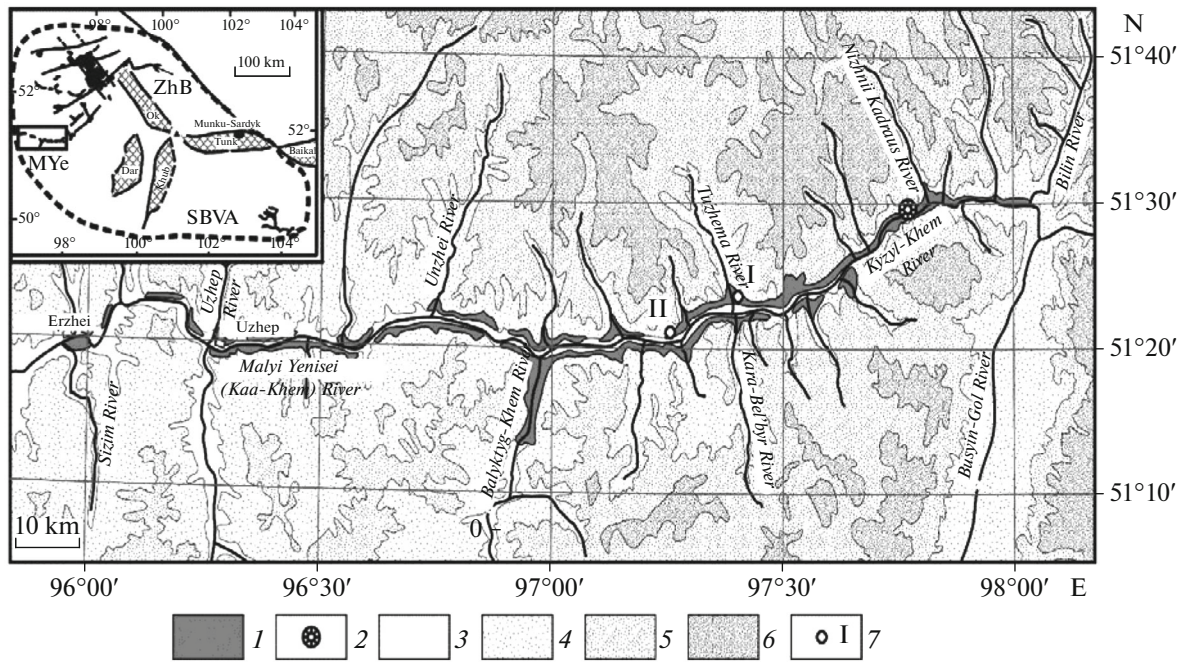
Fig. 2. The layout of lava flows in Malyi Yenisei river valley according to (Yarmolyuk et al., 2004): *1*, lavas; *2*, eruption center; *3—6*, topography elevation levels (*3*, <1000 m; *4*, 1000−1500 m; *5*, 1500−2000 m; *6*, >2000 m); *7*, sampling sites. Inset: positions of Malyi Yenisei (MYe) and Zhom-Bolok (ZhB) lava rivers in system of Late Pliocene−Holocene volcanic fields of the South Baikalian volcanic area (SBVA).

samples was carried out in parallel in two laboratories: in the Laboratory of the Main geomagnetic field and rock magnetism of the Schmidt Institute of Physics of the Earth of the Russian Academy of Sciences (IPE RAS) in Moscow and in the Paleomagnetic Laboratory of Kazan Federal University. In Moscow, TMA was conducted on a (thermo) vibromagnetometer designed by N.M. Anosov and Yu.K. Vinogradov, and in Kazan, on Curie (thermo)magnetic balance designed by B.V. Burov and P.G. Yasonov. We note that these instruments significantly differ in terms of the mass (and volume) of the studied samples which is 2−2.5 g for a vibromagnetometer in Moscow and ~0.1 g for the Curie balance in Kazan. Both instruments have approximately equal specific magnetization sensitivity of ~10^{-5} Am^2/kg. The Curie point determination accuracy is ~5°. Given that the specific saturation magnetization M_s of iron at 20°C is 217.5 Am^2/kg (Bozorth, 1951), the lower measurement threshold of iron concentration for both instruments is ~10^{-5} wt %.

TMA is the continuous measurements of the magnetic moment M of a sample in a constant magnetic field of 0.6 T (vibromagnetometer) and 0.4 T (Curie balance) under sample's heating in air at a rate of 60°/min from room temperature to 800°C and subsequent cooling to room temperature on a vibromagnetometer and at a rate of 100°/min on the Curie balance.

The typical TMA curves obtained on the vibromagnetometer and Curie balance are shown in Fig. 3.

For estimating iron concentration in the sample, the heating curve $M(T)$ is extended (extrapolated) from the Curie point of native iron (700−780°C) to the Curie point of hematite (670°C) below which the $M(T)$ curve typically substantially changes because of the presence of hematite, magnetite and other magnetic minerals with lower Curie points in the sample. The difference ΔM between the extrapolated curve and the heating curve at 670°C normalized to the sample's mass m is a quantity that is close to the specific saturation magnetization M_s s of iron in the sample since the thermomagnetic measurements were carried out in a saturation magnetic field for iron. The experience of TMA shows that the magnetization ΔM obtained in this way does not differ significantly from that estimated from curve extrapolated to room temperature. The difference is even less significant if we take into account that the concentration of iron in the studied basalts is frequently below 10^{-4}%. The ratio of $\Delta M/m$ to the specific saturation magnetization of pure iron (217.5 Am^2/kg) gives the approximate relative content of iron in the sample.

Of course, the accuracy of this determination of iron concentration in a sample is low but it is quite sufficient considering the fact that iron concentration in the studied rocks varies within orders of magnitude. We note that insufficient accuracy of TMA in concentration determination is counterbalanced by the simplicity of the method itself and by the simple proce-
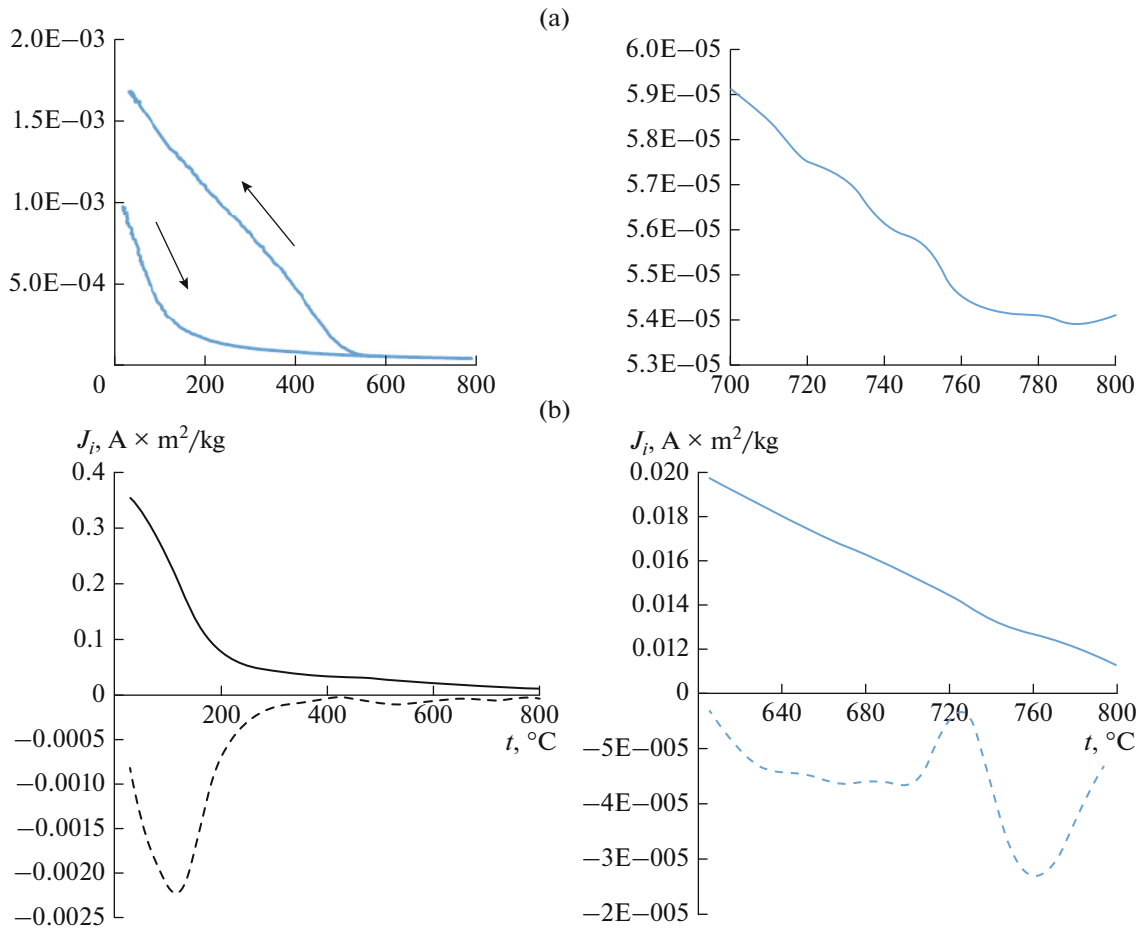
(a)

(b)

J_i, A × m²/kg

J_i, A × m²/kg

t, °C

t, °C

Fig. 3. Typical TMA curves obtained on (a) vibromagnetometer and (b) Curie balance. Right: enlarged TMA curve fragments in vicinity of Curie temperature of iron.

dure of sample preparation for measurements as well as by rapid and mass obtaining the results

RESULTS OF THERMOMAGNETIC MEASUREMENTS

Figures 3−5 and 7−9 show the histograms illustrating the distribution of the number of studied samples
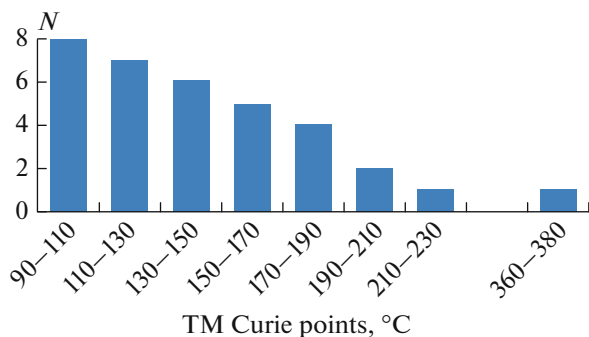

Fig. 4. Histogram of titanomagnetite Curie points in Malyi Yenisei basalts.

by a certain parameter determined in TMA (the Curie point, concentration, etc.). On the ordinate axis in these figures, the number of samples N with a certain parameter value is everywhere. We will call these figures simply *histograms or parameter distributions* (Curie points, concentration, etc.).

The TMA of the samples of MYe basalts has shown that the main carrier of magnetization in the studied basalts is primarily magmatic titanomagnetite (Figs. 4, 5) with the Curie points of 100−120°C which correspond to a depth of the source magma chamber of ~60 km (55−65 km) (Pechersky and Didenko, 1995).

The form of the histogram for the distribution of samples by the Curie points (T_c) of titanomagnetites (TM) with a gradual decrease in N with increasing T_c (Fig. 4) is due to the single-phase oxidation of primary magmatic titanomagnetite. The subsequent heterophase oxidation of titanomagnetite leads to the formation of a mineral close to magnetite and to the disintegration of titanomagnetite. The latter is clearly illustrated in Fig. 5 where against the background normal distribution of TM concentration with a mode of 0.5−0.7%, an "anomalous" zero group of samples is
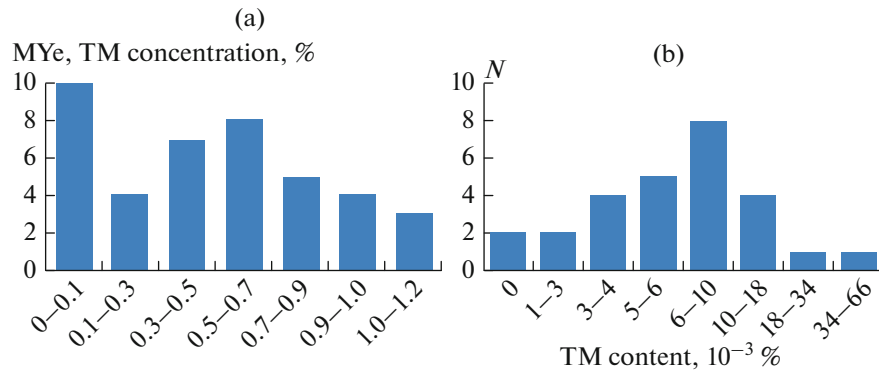
Fig. 5. Histograms of titanomagnetite concentration in basalts of (a) Malyi Yenisei and (b) Zhom-Bolok.

observed in which TM is absent because of its secondary oxidation. Interestingly, a similar significant zero group is not observed in the Zhom-Bolok basalts (Fig. 5b), i.e. the latter are noticeably less oxidized than the MYe basalts; therefore, the histogram of titanomagnetite concentrations in the Zhom-Bolok basalts is closer to the true one.

The samples containing titanomagnetite are marked by a noticeable increase in the saturation magnetization after heating the sample to 800°C (Fig. 6) due to the TM oxidation with the formation of magnetite. In the samples that underwent heterophase oxidation in their initial state (before the laboratory heating at TMA) and contain a magnetic mineral close to magnetite, magnetization does not increase after heating and even decreases. The explanation is that the laboratory heating to 800°C causes oxidation of some part of magnetite to hematite due to which the magnetization after heating decreases (left column in Fig. 6).

This is an important point because samples that underwent in situ heterophase oxidation and do not contain titanomagnetite but only magnetite, very frequently do not also contain metallic iron which, perhaps just as titanomagnetite, has been destroyed a result of natural oxidation of basalt (Table 1). Here, the correlation between the concentrations of titanomagnetite and iron is absent, which is emphasized by the very low correlation coefficient between concentrations of TM and iron (−0.045). The data presented in Table 1 show apparent correlation between concentrations of iron and TM associated with equal influence of oxidation on iron and titanomagnetite.

In the MYe basalts, just as in all the other studied terrestrial and lunar objects, iron is predominantly close to pure with $T_c > 760$°C (Fig. 7). However, compared to the other magmatic objects shown in Fig. 7, iron particles from MYe and Zhom-Bolok basalts contain largest amount of impurities which is expressed in a more significant contribution of the Curie points of 720−750°C (Fig. 7a, 7b). On the other hand, the Curie points of 775°C and higher are likely to be due to the small admixture of cobalt in iron.

Let us consider the distribution of iron concentration in the vertical cross section of each MYe lava flow based on TMA data (Fig. 8) in some more detail.

In liquid basaltic lava, heavy particles of metallic iron should sink, just as reflected in the obtained data presented in Fig. 8 and Table 2. Figure 8, though, shows only the overall trend of iron concentration increasing from the top down the lava flow, most clearly manifest in the MYe-1, 3, 5 flows. This trend is violated in the MYe-4, 6 flows and completely absent in the MYe-2 flow (Fig. 8).

In the thickness intervals of the four flows listed in Table 2, the gradients of the increase in iron concentration from top down the section are fairly close which testifies in favor of the decisive role of gravity (constant acceleration of gravity) in iron particle deposition in liquid lava. We note that in the other intervals of the flows' thickness (not shown in Table 2), a regular increase in iron concentration from top downwards is absent which is perhaps associated, inter alia, with a noticeable difference of lava motion from laminar. Of course, large scatter of the results and the absence of a regular increase in iron concentration from top downwards can also be caused by a trivial factor, namely, a very low iron content in samples, close
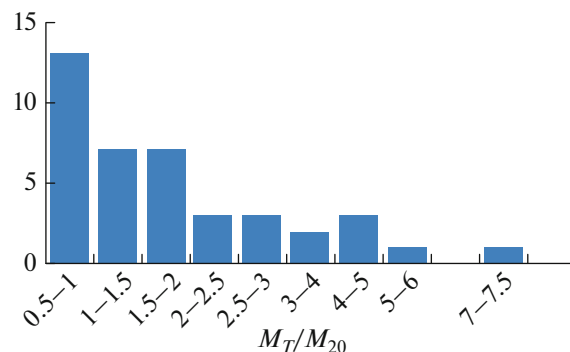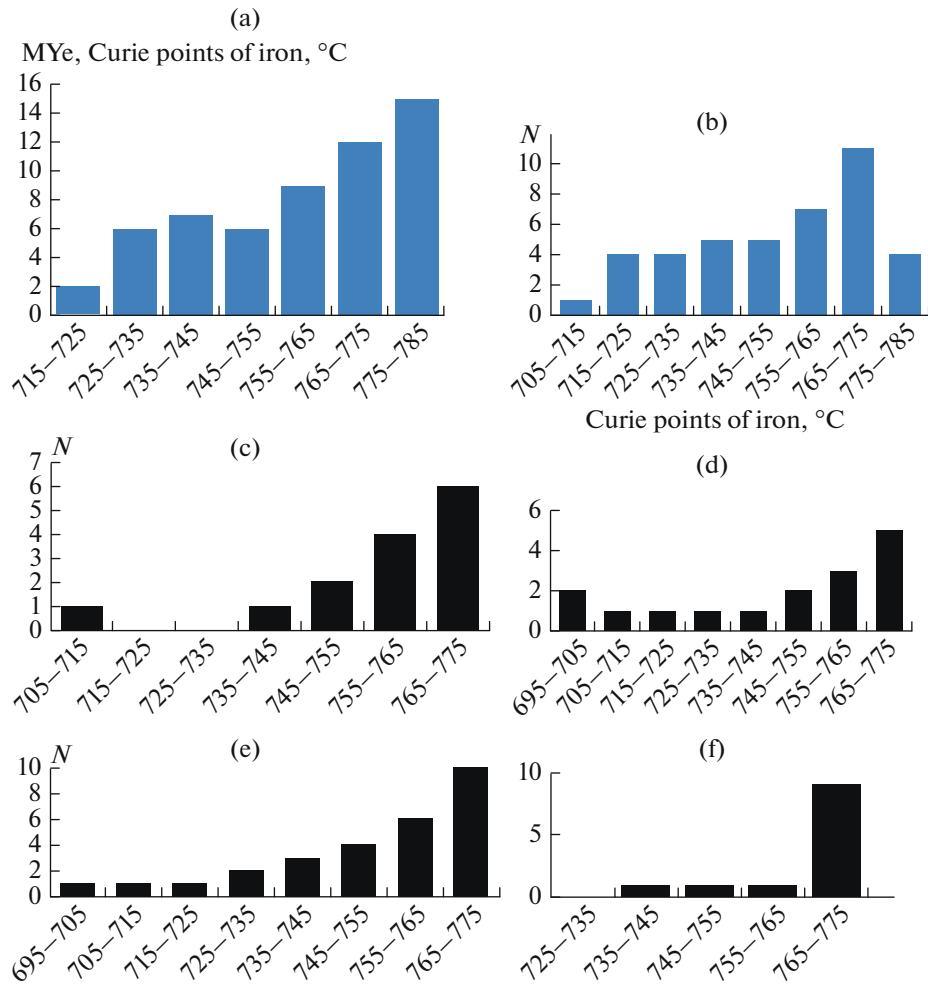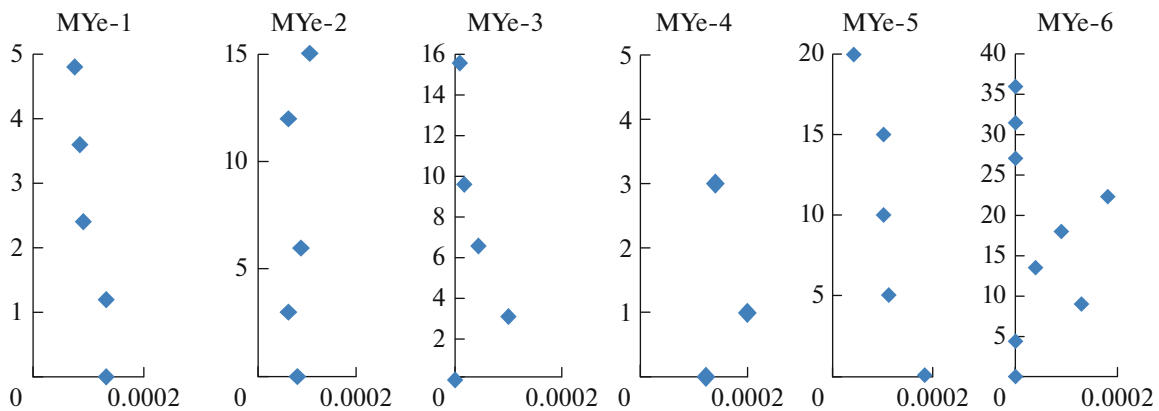

Fig. 6. Histogram of saturation magnetization ratio after sample's heating to 800°C (M_T) to initial value (M_{20}).

Fig. 7. Histograms of Curie points of iron in basalts of (a) Malyi Yenisei; (b) Zhom-Bolok; (c) in hyperbasites from different regions; (d) in Siberian traps; (e) in oceanic basalts from different regions (Pechersky et al., 2017); (f) in lunar basalts (Nagata et al., 1974).

Fig. 8. Iron vertical distribution in six lava flows of Malyi Yenisei. Abscissa axis is iron concentration in %, ordinate axis is vertical thickness of flows in m. (Zero results where titanomagnetite and iron are absent probably due to decomposition by secondary oxidation are not shown.)

to the sensitivity threshold of the measuring instruments and, accordingly, large errors in the determination of iron concentration in the MYe basalts.

It was noted above that TMA of the samples of MYe basalts was conducted in parallel on the twin samples in two laboratories where the studied samples

Table 1. Apparent correlation between iron concentration and titanomagnetite concentration in basalts

TM content, %	C_{Fe} range, 10^{-3}, %	Mean C_{Fe}, 10^{-3}, %	Number of samples without iron
0–0.05	0–0.13	0.037 ($N = 20$)	11
0.06–1.2	0–0.20	0.102 ($N = 18$)	3

Table 2. Growth gradient of iron concentration C_{Fe} from top downwards in selected thickness intervals of three lava flows of Malyi Yenisei basalts (Fig. 7)

Lava flow	Flow thickness interval with increasing C_{Fe}, m	Difference $C_{Fe} \times 10^{-5}$, % C_{Fe} (bottom)−C_{Fe} (top)	Growth gradient $C_{Fe} \times 10^{-5}$, %/m
MYe-1	2.4–1.2	2	1.7
MYe-3	9.0–3.3	9	1.6
MYe-5	5.0–0	9	1.8

Table 3. Iron concentration C_{Fe} in different magmatic objects

Object	C_{Fe} range, 10^{-3}, %	Number of samples	Mean C_{Fe}, 10^{-3}, %
Oceanic basalts	0–18.0	21	1.2
Siberian Traps	0–5.5	37	0.61
Hyperbasites	0–3.0	45	0.18
Zhom-Bolok basalts	0–0.5	28	0.07
Malyi Yenisei basalts (2.5 g)	0–0.4	39	0.09
Malyi Yenisei basalts (0.1 g)	0–0.9	39	0.08

noticeably differed in mass and size. Apparently, it would be interesting to compare the TMA data on iron concentration obtained in two laboratories, i.e. in two variants of sample's size and mass: ~2.5 g (Fig. 9a) and ~0.1 g (Fig. 9b).

In the case of "large" samples (Fig. 9a), for iron, just as for titanomagnetite, two groups of samples are distinguished in the histograms. The first group has a low (almost zero) iron concentration ranging from 0 to 0.00002% and incorporates samples with a noticeable secondary oxidation. The second group is related to titanomagnetite samples and, obviously, it reflects the true iron distribution in basalts, it is lognormal, the mode is 0.00008–0.00016%. We note that in the Zhom-Bolok basalts in which the degree of secondary oxidation of both titanomagnetite and iron is substantially lower, the distribution of iron content is unimodal and close to lognormal with a mode of 0.003–0.004% (Fig. 9c).

Quite a different situation is observed for the "small" samples (Fig. 9b) in half of which iron is completely absent and in the other samples randomly scattered single occurrences of low iron concentration ranging between 0.00001 and 0.0009% are detected, reflecting the uneven distribution of iron in basalts where the distance between iron particles can be commensurate with the size of "small" samples. Correspondingly, correlation between iron concentrations in the "large" and "small" samples is absent, the cor-

relation coefficient is $r = -0.024$. At the same time, mean concentrations of iron in the "small" and "large" samples are practically identical: 0.00009 and 0.00008% (Table 3).

The composite data on iron concentration in the different magmatic formations in the different regions of Russia presented in Table 3 show fairly wide variations among different objects both in the limiting values and in the mean values. The maximum iron concentrations are observed in oceanic basalts, lower concentrations in the Siberian traps and hyperbasites, and minimal concentrations in the Zhom-Bolok and Malyi Yenisei basaltic lavas (Table 3).

A remarkable feature is that the particle size histograms of iron grains in the different rocks are similar (Fig. 10). This similarity is most clearly expressed in the same particle size modes (10–20 μm). The fact that the particle size distribution and the particle size mode do not depend on the origin and age of the rocks (young oceanic basalts, Permian–Triassic traps, ancient hyperbasites) as well as on the type of the source of particles (terrestrial or extraterrestrial) is especially important.

In our opinion, only one factor determining the observed distribution can explain this result: this is the Earth's gravity. Therefore, from the particle size histogram of iron particles (particle size mode), it is apparently possible to reconstruct gravity or, to be more pre-
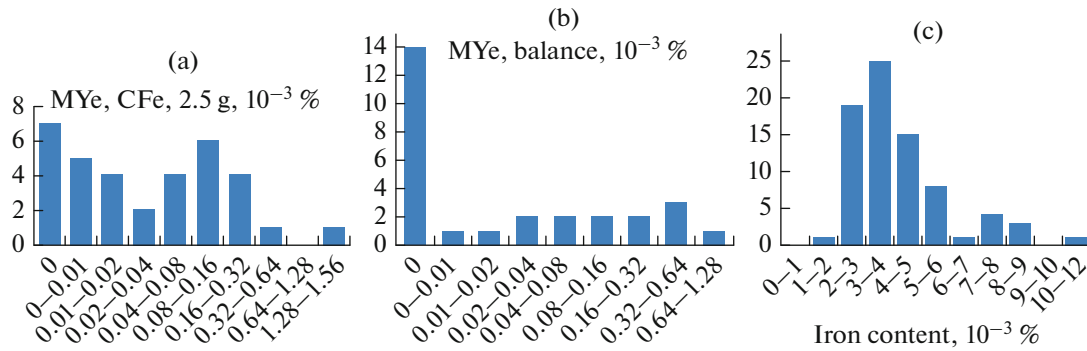
Fig. 9. Histogram of metallic iron concentration in samples of Malyi Yenisei basalts with mass (a) ~2.5 g and (b) ~0.1 g; (c) in Zhom-Bolok basalts (c).
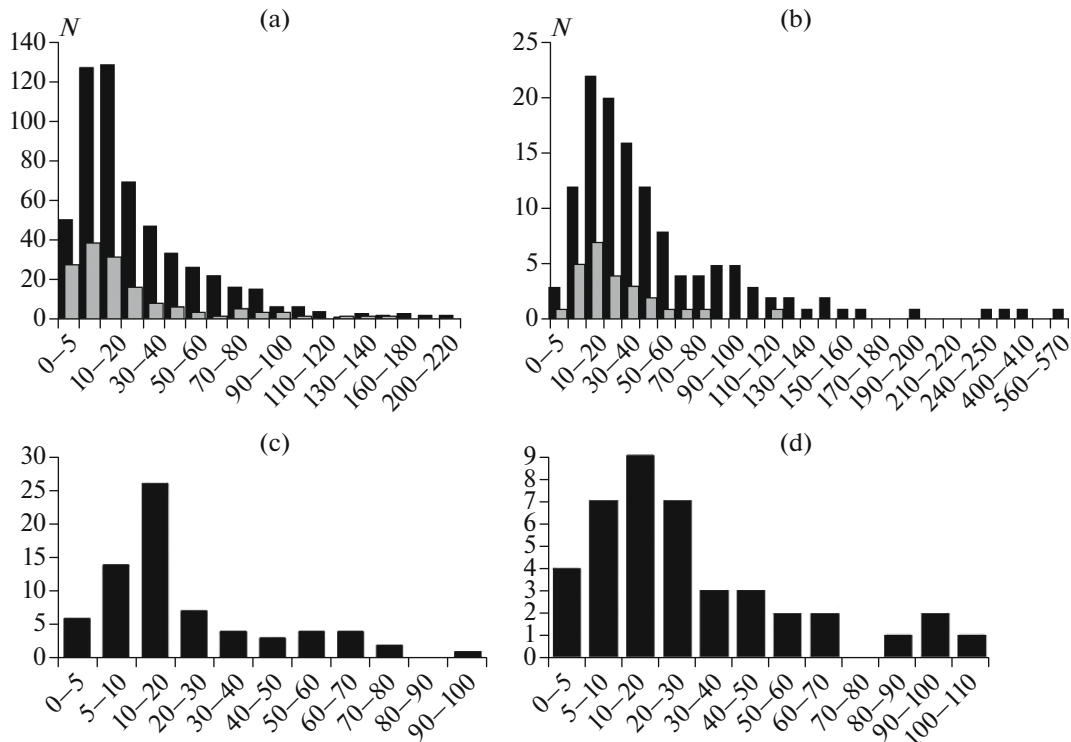
Fig. 10. Particle size histograms of native iron (in microns) containing (gray) and not containing (black) nickel admixture in (a) sediments, (b) hyperbasites, (c) traps and (d) oceanic basalts (Pechersky, 2015 ; Pechersky et al., 2017).

cise, gravitational acceleration, and, hence, the mass of the planet—the source of iron particles in both the basaltic lava and sediments.

It is worth noting that in this case, particle size of iron is determined in a thin section; therefore, the iron particle size information does not largely depend on secondary alteration of iron grains, in contrast to the Curie points which substantially depend on the degree of preservation of the material and on iron particle concentration. This offers a unique possibility to track the value of gravitational acceleration on the Earth over a long period of time, for example, 3−4 billion

years, based on the data on the average size of iron particles.

For assessing the dependence of the size mode of iron particles on gravitational acceleration, it is necessary to model the grain size distribution of iron particles in exactly identical liquid media that only differ by different gravitational accelerations, i.e., different sizes (masses) of planets—sources of iron particles. The next step is to construct the described histograms from the samples available for measurements, e.g., from the Moon ($g = 1.62$ m/s^2), Mars (3.71 m/s^2), Earth (9.807 m/s^2), from the asteroid belt (stone mete-

orites), and, thus, to relate the particle size mode of iron with gravitational acceleration.

CONCLUSIONS

In liquid basaltic lava, heavy particles of metallic iron should sink, which is exactly what we observed in several thickness intervals of the flows of the Malyi Yenisei lava river, despite the large scatter of the results caused by various factors including a noticeable deviation of lava motion from laminar, secondary oxidation of iron grains, etc. In a number of thickness intervals of lava flows, the gradients of the increase in iron concentration from top down the flows are very close $(1.6-2 \times 10^{-5}\%/m)$, which is likely to testify in favor of the decisive effect of gravity leading to the deposition of iron particles in liquid lava. Meanwhile, based on gravity (gravitational acceleration), it is, in principle, possible to estimate the mass of the planet that is the source of iron particles!

Unfortunately, in this approach to estimating the mass of the planet, we are faced with a problem that is as of now unsolvable: how could we get lava flow sequences of the source planets of iron particles? However, an alternative solution can help: mass of the planet can be estimated from the grain size histogram of iron particles or, more simply, from its mode, which can be obtained based on individual samples of basalts, terrigenous sediments, stone meteorites, and, which is very important, almost irrespective of the degree of their preservation. Future research will address the solution of this problem—establishing the correlation between particle size mode and gravitational acceleration.

REFERENCES

Bozorth, R.M., *Ferromagnetism*, New York: D.Van Nostrand Comp., 1951.

Nagata, N., Sugiura, N., Fisher, R.M., Schwerer, F.C., Fuller, M.D., and Dunn, J.R., Magnetic properties of Apollo 11−17 lunar materials with special reference to effects of meteorite impact, *Proc. 5th Lunar Conference*, 1974, vol. 3, pp. 2827−2839.

Pechersky, D.M., *Raspredelenie chastits samorodnogo zheleza i Fe-Ni splavov na planetakh* (Distribution of Native Iron Particles and Fe-Ni Alloys on Planets), Saarbrücken: Palmarium Acad. Publishing, 2015.

Pechersky, D.M. and Didenko, A.N., *Paleoaziatskii okean* (Paleo-Asian Ocean), Moscow: OIFZ RAN, 1995.

Pechersky, D.M., Kazansky, A.Yu., Kozlovsky, A.M., Markov, G.P., Shchetnikov, A.A., and Tselmovich, V.A., Basalts of the Zhom-Bolok lava river as a possible sources of metallic iron in sediments of local lakes: thermomagnetic and microprobe justification, *Int. Conf. on Paleomagnetism and Rock Magnetism*, Russia, Kazan, 2017.

Pechersky, D.M., Markov, G.P., Kuzina, D.M., and Tsel'movich, V.A., Native iron in the Earth and space, *Izv. Phys. Solid Earth*, 2017, vol. 53, no. 5, pp. 658−676.

Pechersky, D.M., Markov, G.P., Tselmovich, V.A., Kazanskii, A.Yu., and Shchetnikov, A.A., Unique phenomenon of the accumulation of terrestrial metal iron particles in lacustrine deposits: Zhombolok volcanic region, East Sayan, *Izv. Phys. Solid Earth*, 2018, vol. 54, no. 1, pp. 106−120.

Yarmolyuk, V.V., Arakelyants, M.M., Lebedev, V.A., Ivanov, V.G., Kozlovskii, A.M., Lebedev, V.I., Nikiforov, A.V., Sugorakova, A.M., Baikin, D.N., and Kovalenko, V.I., Chronology of valley eruptions in the South Baikal volcanic region: Evidence from K-Ar dating, *Dokl. Earth Sci.*, 2003, vol. 391, no. 5, pp. 636−640.

Yarmolyuk, V.V., Kozlovskii, A.M., Kudryashova, E.A., Lebedev, V.I., and Sugorakova, A.M., Major valley lava flows in Asia during the Cenozoic: structure, composition, and the environment of the "Lava river" forming in the Malyi Yenisei river valley, *Vulkanol. Seismol.*, 2004, no. 4, pp. 3−20.

Yarmolyuk, V.V., Kudryashova, E.A., Kozlovsky, A.M., Lebedev, V.A., and Savatenkov, V.M., Late Mesozoic−Cenozoic intraplate magmatism in Central Asia and its relation with mantle diapirism: Evidence from the South Khangai volcanic region, Mongolia, *J. Asian Earth Sci.*, 2015, vol. 111, pp. 604−623.

Translated by M. Nazarenko